Polymer Bulletin (2021) 78:5567–5591
https://doi.org/10.1007/s00289-020-03379-x

ORIGINAL PAPER

Effect of the multi-functional epoxides on the thermal, mechanical and rheological properties of poly(butylene adipate-co-terephthalate)/polylactide blends

D. D. Wu[1,2] · Y. Guo[1] · A. P. Huang[1] · R. W. Xu[1] · P. Liu[2]

Received: 4 December 2019 / Revised: 4 September 2020 / Accepted: 23 September 2020 /
Published online: 6 October 2020

Abstract

The growing interest for biodegradable products promoted the development of new materials. In this work, three types of multi-functional epoxides of Joncryl ADR4368, ADR4380 and ADR4370 were used to study the effect of Joncryl types on the morphology, mechanical, thermal and rheological properties of poly(butylene adipate-co-terephthalate)/poly(lactide) (PBAT/PLA) blends. According to the structure information of ADRs, the reaction mechanism between different ADRs with PBAT and PLA was the same. The results of GPC, mechanical, rheological properties and DSC indicated that PBAT/PLA/ADR4368 blends showed the high M_n, mechanical properties, viscoelasticity and good compatibility compared with PBAT/PLA/ADR4380 and PBAT/PLA/ADR4370 blends. The performance difference of PBAT/PLA/ADR4368, PBAT/PLA/ADR4380 and PBAT/PLA/ADR4370 blends mainly derived from the different amount epoxy reactive functional groups per molecule. ADR4368 had the best modification effect. When the content of ADR4368 reached 0.2 wt%, the tensile strength of the PBAT/PLA/ADR4368 blend increased by about 10 MPa and without any loss in elongation at break compared with that of PBAT/PLA blend. The compatibility between the PBAT and PLA was significantly improved by in situ formation of the graft/comb PBAT-*g*-PLA copolymers in the presence of the ADR4368, resulting in the enhancement properties of the blends. In addition, thermogravimetric analysis showed enhancement in the thermal stability for the PBAT/PLA/ADR blends.

Keywords PBAT · PLA · Compatibilization · Properties · Morphology

✉ R. W. Xu
xurenwei@petrochina.com.cn

✉ P. Liu
pliu@lzu.edu.cn

[1] Lanzhou Petrochemical Research Center, Petrochemical Research Institute, Petrochina, Lanzhou 730060, China

[2] College of Chemistry and Chemical Engineering, Lanzhou University, Lanzhou 730000, China

Introduction

The research focus on biobased and biodegradable polymers has seen growing interest in the recent years because of the continual environmental concerns, as well as because of the risks of depletion of fossil fuels which provide the raw materials for most of the conventional polymers [1–3]. In recent years, a variety of biodegradable polymers have already been introduced into the market and can compete with non-biodegradable traditional polymers in different applications (packaging, biomedical, textile, etc.). In particular, the large use of plastics in the film industry has increased the interest in using biodegradable polymers to replace conventional polymers in order to reduce the influence on environment due to the inappropriate disposal.

PBAT is a biodegradable and biocompostable aliphatic–aromatic copolymer with high flexibility, thermal stability and biodegradability as well as good processing properties. The mechanical behavior of PBAT was similar to a thermoplastic elastomer. The main drawback of PBAT was the low stiffness. PBAT was initially designed by BASF with the trademark "Ecoflex®." Nowadays, it has been widely used in the production of blown film, such as packaging and membrane products [4, 5].

Poly(lactic acid) (PLA) is one of the most extensively studied biobased and biodegradable aliphatic polyester. Firstly, lactic acid is produced from various starches, sugars, and other biomass materials through biological fermentation and then is chemically converted to poly(lactic acid) [6]. PLA has high strength and stiffness at room temperature and can be processed like conventional plastics. These favorable properties make PLA as a promising substitute for conventional petroleum-based polymers. In recent years, PLA has been widely used in the development of packaging and biomedical industry applications [7]. However, the wide application of PLA is still limited mainly by its brittleness [8, 9]. Many methods have been investigated to improve the toughness of PLA such as plasticization [10], copolymerization [11–14] and blending with a variety of flexible polymers [15–21]. Among these methods, blending PLA with ductile and biodegradable polymers presented a more practical prospect. Moreover, in view of its high toughness and biodegradability, combining PBAT with PLA has been considered the most promising advantages because of the complementary properties between the high toughness of PBAT and the high strength of PLA [22, 23]. Chiu et al. [24] reported that adding 30 wt% PBAT into PLA, the elongation at break increased from 3.0% to about 25.0%, while the tensile strength reduced from 58.0 to 43.0 MPa, respectively. When the further increase in the content of PBAT up to 50 wt%, the elongation at break of the blend increased to 50.0%, while the tensile strength reduced to 30.0 MPa. These results suggested that the brittle deformation behavior of the PLA was improved after blending proper amounts of PBAT in the PLA matrix. Although the melt blending PLA with PBAT can improve the complementary properties for the PBAT/PLA blends, the improved ratio of elongation at break was low and the reduced ratio of tensile strength was high. In other words, the blending sacrificed the tensile strength of PLA remarkably, but

increased the elongation at break slightly. The most important factor influencing the properties of PBAT/PLA blends was their mutual miscibility [25, 26].

Yeh et al. [27] studied the miscibility between PBAT and PLA. The study found that PBAT molecules were miscible with PLA molecules in the case of the content of PBAT was less than 2.5 wt%, but phase-separated droplets can be distinguished above this amount. The typical 'sea-island' morphologies of PBAT/PLA blends were common in the documents [23, 28], indicating that miscibility between PLA and PBAT is limited. Usually, the PBAT/PLA blend was considered as the immiscible pairs. There are numerous defects in the immiscible polymer blends often leading to poor mechanical properties [24, 29]. Therefore, developing good interface compatibility between PLA and PBAT was essential to obtain a blend with satisfactory properties [30]. The compatibilization can be performed by introduction of premade copolymers or in situ reaction through the possible reactive functional groups. The in situ compatibilization can be happened by using dicumyl peroxide (DCP) inducing free-radical reaction [31, 32] or using a chain extender with multifunctional groups that can react with both carboxyl and hydroxyl groups during the processing of PLA and PBAT [33–35].

Branching/crosslink represented a successful approach to improve interfacial adhesion in multiphase materials. Indeed, branching/crosslink triggered the emerging of mixed chains (copolymers), which acted as compatibilizers at the interphases. Many examples were reported in which free radical promoted branching/crosslink of immiscible biodegradable polyesters resulting in successfully tuned mechanical properties. The PLA/PBS blends [15], PLA/PCL blends [18] and PLA/PBAT blends [36] have been successively prepared via in situ compatibilization with the addition of a small amount of DCP. The notched Izod impact strength and the tensile strength of these blends were higher than that without DCP. However, the use of DCP as the reactive compatibilizer can cause some extent of degradation reaction and DCP was harmful to the environment during processing. The use of chain extenders was an alternative to improve the compatibility of these blends. This method was effective and appropriate to mass production by reactive extrusion. The chain extenders with epoxy groups were effective compatibilizers for PBAT/PLA blends, which can form PLA-*g*-PBAT copolymers and enable re-linking the broken polymer chains due to the thermal degradation reaction under the process condition. Kumar et al. used glycidyl methacrylate (GMA) as a reactive compatibilizer for the PBAT/PLA blends. The results showed that the toughness of the PLA/PBAT blends was improved with the content of 3–5% GMA [37]. Dong et al. used different chain extenders (Joncryl ADR-4370S abbreviated as ADR and 1,6-hexanediol diglycidyl ether abbreviated as HDE) with multi-epoxy groups to compatible PLA and PBAT. The compatibility between the PLA and PBAT was significantly improved by in situ formation of PLA-*g*-PBAT copolymers in the presence of the chain extenders. Ultimately, the ductility of the blends enhanced significantly. The elongation at break was increased from just over 200% of PBAT/PLA (20/80) blend to above 500% by the addition of chain extenders at the same time without any decrease in the tensile strength [35].

Recently, the multifunctional styrene-acrylic-epoxy random oligomer (Joncryl ADR) was widely used as chain extenders for biodegradable polymers [33, 34, 38–42]. It could provide a simple and effective way to develop the interfacial region

which was necessary for properties modulation through a mechanism of inter-macromolecular branching or crosslink reactions. Multifunctional chain extenders promoted the formation of copolymers during compounding in the molten state. The copolymers worked as compatibilizers which can increase the interface adhesion and reduce the size of the dispersed phase.

Although many works studied the effect of ADR as chain extender on the properties of PBAT/PLA blends, we had a question which grade of ADR had the excellent properties for the PBAT/PLA blends. ADR is a commercial epoxy-based chain extender supplied by BASF, Germany. It is a modified acrylic copolymer with epoxy function. Different kinds of ADRs were provided by BASF. The documents [35, 40] adopted different types of ADR, which all revealed remarkable improvement in the properties of PBAT/PLA blends. However, the modified effect of different ADRs made a difference for a given polymer system. In this paper, we compared the effect of common ADRs on the properties of PBAT/PLA blends based on reactive melt blending for the industrial package and film applications to lay solid foundation. The weight ratio of PBAT/PLA was designated as 80/20 wt%/wt%. PBAT was the main composition for potential flexible plastic film applications. The phase morphology, mechanical properties, thermal properties and rheological properties of the modified and unmodified PBAT/PLA blends were studied in detail.

Experimental

Materials

PBAT was supplied by Xinjiang Blue Ridge Tunhe Polyester Co, Ltd. The weight-average molecular weight was 132,421 g/mol, and the polydispersity index was 1.81 determined by GPC measurements. PLA, grade 2003D, was a commercial available polyester purchased from NatureWorks LLC, USA. It had the weight-average molecular weight of 219,355 g/mol and polydispersity index of 1.41 obtained from GPC measurements. A series of Joncryl ADRs (abbreviated as ADR) as chain extenders were supplied by BASF. The chain extenders were ADR4368, ADR4380 and ADR4370, and the general information was provided by the supplier. Molar mass of ADR was typically of the order of 7000 g/mol, and it contained 5 to 10 epoxy reactive functional groups per molecule. The basic information conformed to the relevant literature [43]. The chemical structure of ADR is shown in Fig. 1.

Blend preparation

PBAT and PLA were dried at 70 °C for 24 h in an oven before processing. All the PBAT/PLA blends were prepared by melt mixing with a Haake Rheomix40 (Karlsruhe, Germany) at a rotating speed 50 r/min at 170 °C for 6 min. The mixing composition of the PBAT/PLA blend was 80/20 wt%/wt%. A certain amount of ADRs was introduced into PBAT/PLA blend. The weight percentage of ADRs was 0.1, 0.15, 0.2, 0.3 and 0.5 wt%, respectively, which represented the amount of ADRs

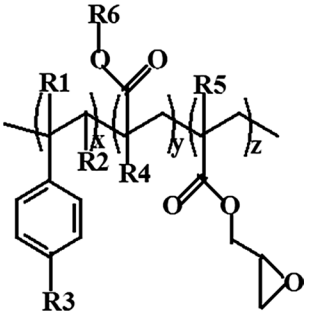

Fig. 1 General structure of the multi-functional oligomeric chain extender family Joncryl; R1-R5 are H, CH_3 or higher alkyl group; R6 is an alkyl group; and x, y and z are each between 1 and 20

per hundred PBAT and PLA resin. After mixing, all of the compounds were cut into small pieces. Then, all of samples were compression molded into sheets with thickness of 1.0 mm at 170 °C, a hold pressure of 10 MPa and a hold time of 3 min, followed by quenching to room temperature between two thick-metal blocks. The specimens were then sealed in plastic bags awaiting the analysis.

Characterizations

^{1}H NMR

^{1}H NMR spectra were recorded using a Bruker AV400 spectrometer (Germany) in $CDCl_3$ at room temperature.

Gel permeation chromatography (GPC)

The measurements of number- and weight-average molecular weights (M_n and M_w) and the molecular weight distribution (M_w/M_n) were taken by GPC measurements on a waters GPC system. Tetrahydrofuran (HPLC grade) (flow rate of 1.0 mL/min) was used as eluent at 35 °C. Monodispersed polystyrene standards obtained from Waters Co. were used to generate the calibration curve. The dilute sample solution was filtrated carefully to remove possible insoluble substance before it was injected into GPC column.

Differential scanning calorimetry (DSC)

Thermal behavior of the blends was studied by DSC (NETZSCH Instruments DSC 214 Polyma Germany) under N_2 atmosphere. The sample weights varied between 5 and 8 mg. All the samples were heated from room temperature to 180 °C at a heating rate of 10 °C/min, holding for 3 min to erase previous thermal history. Then they were cooled to −50 °C at a cooling rate of 10 °C/min (first cooling), and subsequently, the second heating scan was performed between −50 °C and 180 °C at a heating rate of 10 °C/min to present the subsequent melting behavior (second heating). The basic data of glass transition temperature (T_g), the melting temperature (T_m), the cold crystallization temperature (T_{cc}) and the melt enthalpy (ΔH_m), crystallization enthalpy (ΔH_{cc}) of

the samples were obtained from the second heating run. The melt crystallization temperature (T_c) and corresponding crystallization enthalpy (ΔH_c) of the samples were obtained from the cooling run.

Mechanical tests

An Instron 5566 tensile testing machine was used to study the static mechanical properties of neat PLA, neat PBAT and PBAT/PLA blends at a crosshead speed of 50 mm/min according to GB/T1040-2006 (China). All dumbbell-shaped specimens cut from the sheets with a total length of 50 mm and a valid testing area of 20×4 mm^2 were subjected to tensile tests at 25 °C after storing for over 24 h under the test conditions, and at least five tests were undertaken for each specimen to calculate average values.

Scanning electron microscopy (SEM)

The morphological feature of the samples was observed by field emission SEM (Zeiss Ultra Plus, Germany) at an accelerating voltage of 5 kV. The samples were fractured by immersion in liquid nitrogen for about 10 min. A layer of gold was sputter-coated uniformly over the sample surface before SEM observation.

Rheological tests

Dynamic rheological measurements of the samples were taken on a rheometer (AR 2000ex USA). Frequency sweep for all samples was adopted using 25-mm plate-plate geometry, and the temperature was set at different points, including 160, 170, 180 and 190 °C. The sheet samples were about 1.0 mm in thickness, and the strain value was fixed at 1.25% in the linear viscoelastic range. The oscillatory frequency sweep was carried out at angular frequency range of 0.1–100 rad/s.

Thermogravimetric analysis (TGA)

TGA was performed using a TGA-Q500 simultaneous thermal analysis instrument (USA). All samples with about the weight of 10 ± 0.2 mg were heated from 50 to 800 °C at 10 °C/min in the nitrogen atmosphere.

Extraction in chloroform

The gel content of the PBAT/PLA blends was obtained by extraction in boiling chloroform for 24 h using a Soxhlet extractor. About 0.2 g of the samples was cut into small pieces and wrapped in a preweighed filter paper. After the extraction, the extracted samples were vacuum-dried to a constant weight. The gel fraction was calculated as follows:

$$\text{gel fraction} = (m_d/m_o) \times 100\%$$

where m_o is the original weight of samples and m_d is the weight of dry residues obtained after extraction.

Results and discussion

^{1}H NMR analysis and gel content

ADR was a commercial product. As just shown in Fig. 1, it was a modified acrylic copolymer with epoxy functions. The chemical structure of ADR was complicated, including different amounts of x, y and z in the main chain and different groups in side chains. The z was related to epoxy functions. The detailed information was not supplied. We carried out the ^{1}H NMR study on the ADR4368, ADR4380 and ADR4370, and the result is shown in Fig. 2.

As shown in Fig. 2, the character peaks of benzene ring proton of polystyrene at 6.3–7.5 ppm could be observed. The character peaks at around 2.3–3.1 ppm belonged to the protons of $–CH_2–$ and –CH– on the epoxy group. Some other peaks were observed at 0.2–2.0 ppm assignable to protons of the –CH–, $–CH_2–$ and CH_3. The spectral line strength during 2.3–3.1 ppm of ADR4368 was bigger than those of ADR4380 and ADR4370. As we all known, the spectral line strength was proportional to the corresponding number of protons, so we concluded that the main structure of different ADRs was similar, but the amount of epoxy group of ADRs was different. The ratio of the area corresponding to the protons of $–CH_2–$ and –CH– on the epoxy group at 2.3–3.1 ppm and the benzene ring proton of polystyrene at 6.3–7.5 ppm for ADR4368, ADR4380 and ADR4370 was 0.38, 0.18 and 0.17, respectively, which illustrated the ratio of the number of hydrogen in

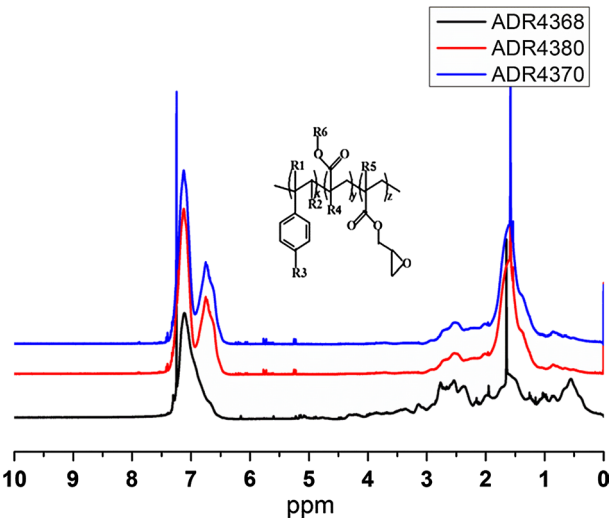

Fig. 2 ^{1}H NMR spectra of ADRs

the epoxy group and the benzene ring proton of polystyrene. According to the above result, the number of the epoxy group of ADR may have the sequence of ADR4368 > ADR4380 > ADR4370.

The gel content was performed for PBAT/PLA/ADR samples. The gel content was obtained by extraction in boiling chloroform for 24 h using a Soxhlet extractor. After the extraction, we found there was no gel detected for all the samples, indicating that there was no crosslink structure in the PBAT/PLA/ADR blends.

GPC analysis

GPC was used to evaluate the molecular weight and molecular weight distribution of the different samples. The M_n, M_w and the molecular weight distribution of the PBAT/PLA blend and PBAT/PLA/ADR blends are summarized in Table 1.

Based on the structural characterization, the reactive mechanism between ADR and PBAT/PLA blend was proposed [33, 40], shown in Fig. 3. The epoxy groups were reactive with –COOH and –OH groups of the PBAT and PLA chains during melt processing. On the other hand, it can recombine the new –COOH or –OH groups which were generated owing to the thermal degradation (random chain scission) during processing at temperature higher than melt temperature. The PLA and PBAT macromolecules were combined together by one molecular of ADR, forming the effective double graft/comb PBAT-*g*-PLA copolymers. The in situ formed copolymers at the interface were responsible for the enhanced compatibility between PBAT and PLA phase. This was an attractive way not only to minimize the degradation effects of PLA and PBAT but also to improve the compatibility.

All the examined samples underwent similar thermal processing. As shown in Table 1, the M_w of PBAT/PLA/0.5ADR4368 blend increased from 142,920

Table 1 Molecular weight analyses of the samples measured via GPC

Samples	M_n	M_w	M_w/M_n
PBAT/PLA	87,106	142,920	1.64
PBAT/PLA/0.1ADR4368	87,021	144,173	1.66
PBAT/PLA/0.15ADR4368	87,055	149,870	1.72
PBAT/PLA/0.2ADR4368	87,111	152,302	1.63
PBAT/PLA/0.3ADR4368	95,083	157,155	1.65
PBAT/PLA/0.5ADR4368	97,071	166,954	1.71
PBAT/PLA/0.1ADR4380	86,300	142,084	1.65
PBAT/PLA/0.15ADR4380	86,389	142,273	1.65
PBAT/PLA/0.2ADR4380	86,664	144,327	1.67
PBAT/PLA/0.3ADR4380	89,732	145,438	1.62
PBAT/PLA/0.5ADR4380	90,716	146,348	1.61
PBAT/PLA/0.1ADR4370	86,145	142,337	1.65
PBAT/PLA/0.15ADR4370	86,461	143,162	1.66
PBAT/PLA/0.2ADR4370	86,989	143,824	1.65
PBAT/PLA/0.3ADR4370	87,163	143,981	1.65
PBAT/PLA/0.5ADR4370	87,923	145,058	1.64

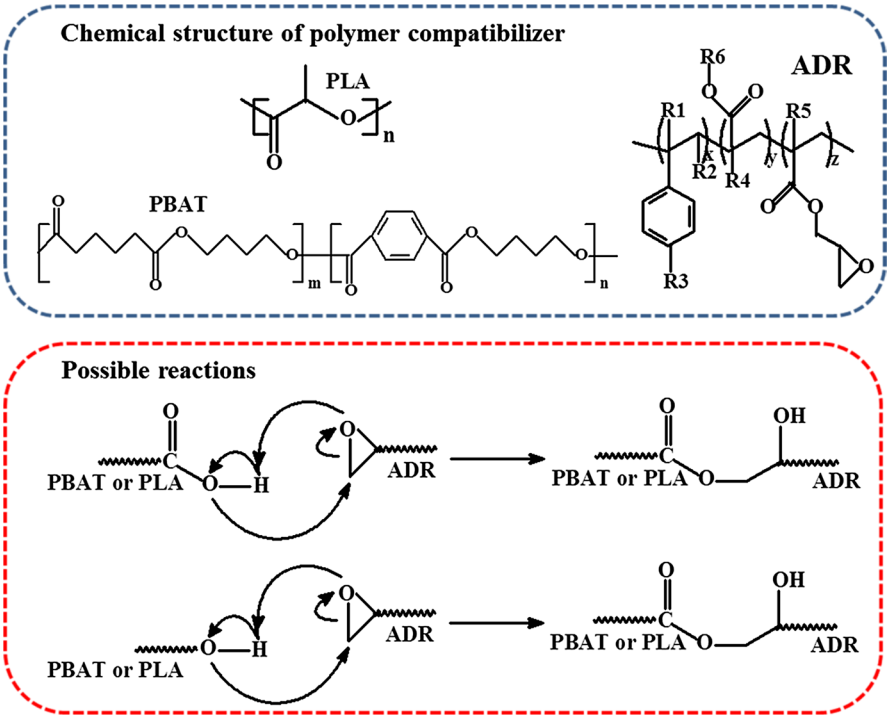

Fig. 3 Possible reactions between PBAT, PLA and ADR during melt blending

for PBAT/PLA blend to 166,954. In the case of PBAT/PLA/0.5ADR4380 blend and PBAT/PLA/0.5ADR4370 blend, the M_w increased to 146,348 and 145,058, respectively. The molecular weight and molecular weight distribution of the different PBAT/PLA/ADR blends changed which can be explained by the mechanisms of conventional branching due to the tethering of the polymer chains to a single ADR molecule, which indicated that chain extension was the main mechanism of the increased molecular weight. Furthermore, it was noted that the PBAT/PLA/ADR4368 blend had a higher molecular weight than that of the PBAT/PLA blend and the corresponding PBAT/PLA/ADR4380 blend and PBAT/PLA/ADR4370 blend because of the stronger chain extension effect of ADR4368. According to the GPC results, the amount of epoxy groups of ADR at given content had the following sequence: ADR4368 > ADR4380 > ADR4370, which was consist with the ^{1}H NMR analysis.

In addition, it had to be remarked that a small amount of non-soluble fraction was observed in the tetrahydrofuran solution of PBAT/PLA/ADR blends in the preparation process of GPC analysis because tetrahydrofuran was not the good solvent for branching PBAT/PLA blends.

Thermal behavior

DSC measurement was taken to study the thermal properties of the PBAT, PLA and PBAT/PLA blends with and without ADRs. Figure 4 shows the DSC curves of the samples, and the corresponding thermal parameters are listed in Table 2.

The T_g and T_m of pure PBAT were −30.2–120.0 °C; on the other hand, the T_g and T_m of pure PLA located at 60.9–150.4 °C, respectively. PLA was a semi-crystalline polymer. The melt crystallization rate of pure PLA was slow, and PLA cannot produce significant melt crystallization at the relatively fast cooling rate of 10 °C/min,

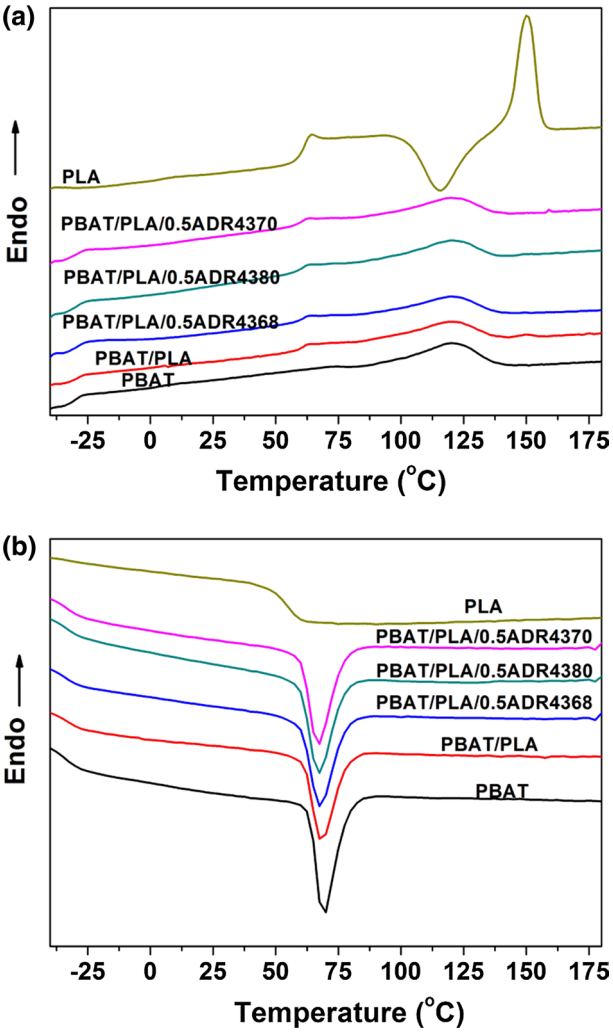

Fig. 4 **a** The second heating curves and **b** the first cooling curves of PBAT/PLA blend and PBAT/PLA/ADR blends

Table 2 Thermal parameters of the pure PBAT, PLA, PBAT/PLA blend and PBAT/PLA/ADR blends

Samples	T_g-PBAT (°C)	T_g-PLA (°C)	T_m-PBAT (°C)	ΔH_m-PBAT (J/g)	T_m-PLA (°C)	ΔH_m-PLA (J/g)	T_{cc}-PLA (°C)	ΔH_{cc}-PLA (J/g)	T_c-PBAT (°C)	ΔH_c-PBAT (J/g)
PBAT	− 30.2		120.0	12.4					68.9	16.8
PLA		60.9			150.4	21.8	115.5	17.9		
PBAT/PLA	− 29.9	61.2	119.9	10.3	149.6	1.0	–	–	68.1	18.0
PBAT/PLA/0.5ADR4368	− 27.5	57.8	119.9	11.5	–	–	–	–	67.4	15.5
PBAT/PLA/0.5ADR4380	− 29.4	60.4	120.0	10.0	–	–	–	–	67.3	17.6
PBAT/PLA/0.5ADR4370	− 30.0	61.4	119.9	10.5					67.1	17.5

ΔH_m and ΔH_c were corrected for the content of PBAT and PLA in the blends

but it can exhibit cold crystallization process at the second heating process. The T_{cc} of pure PLA was observed at approximately 115.5 °C. For the pure PBAT, there was no cold crystallization signal presented in the second heating curve. However, an obvious melt crystallization peak occurred in the cooling cycle and the crystallization proceeded in a narrow temperature range, which indicated that PBAT had a fast melt crystallization rate. In case of the PBAT/PLA blend, the DSC curves revealed two $T_g s$, the higher T_g was corresponding to PLA component, and the lower one was corresponding to PBAT component. Moreover, the T_g of both PBAT and PLA components in the blend showed no shift toward each other, suggesting that PBAT and PLA were immiscible. T_m of PBAT and PLA in the PBAT/PLA blend was 119.9–149.6 °C, and they had no apparent change compared with pure PBAT and PLA. However, the corresponding ΔH_m value of both PBAT phase and PLA phase in the PBAT/PLA blend reduced. This was because the crystallization ability of molecular chains of PBAT and PLA was inhibited due to a reduction in the lamellar thickness resulting from the melt blending. For the PBAT/PLA blend, in the second heating curves, the cold crystallization region of PLA was overlapped with the crystallization melt process of PBAT, and eventually cold crystallization region of PLA was masked by the crystallization melt process of PBAT because of PBAT content up to 80 wt%. Therefore, the reduction in the lamellar thickness of PLA due to the crystallization melt process of PBAT inhibited the regular arrangement of the PLA molecular chains. On the other hand, the reduction in the lamellar thickness of PBAT due to at the T_c of PBAT, PLA had already solidified which inhibited the molecular chain's movement.

T_gs of PBAT and PLA component in the PBAT/PLA/ADR4368 blend shifted toward each other. This proved the improved thermodynamically miscibility between PBAT and PLA by addition of ADR4368 by DSC measurement. However, the T_gs of PBAT and PLA component in the PBAT/PLA/ADR4380 blends and PBAT/PLA/ADR4370 blends were nearly unchanged. This implied thermodynamically immiscibility for PBAT/PLA/ADR4380 blends and PBAT/PLA/ADR4370 blends. The T_c in the PBAT/PLA blend slightly decreased, indicating that the introduction of PLA inhibited melt crystallization capability of PBAT, while the T_c in the PBAT/PLA/ADR blends slightly increased, meaning that the introduction of branching structure promoted the melt crystallization of PBAT [43]. In addition, the T_m of PLA component disappeared when introducing the ADR, regardless of the type of ADR. This can be explained by the effect of chain extension of ADRs decreasing the crystallization capability of PLA.

Mechanical properties

The effect of ADRs on the mechanical properties of the PBAT/PLA blends was studied by tensile test. The tensile mechanical behavior is shown in Fig. 5. As shown in Fig. 5a, it showed an obvious variation tendency of tensile strength for the PBAT/PLA blend and PBAT/PLA/ADR blends. The best enhancement effect was ADR4368. The high enhancement efficiency in tensile strength can be due to the synchronicity of compatibilization due to the formation of PBAT-*g*-PLA copolymers

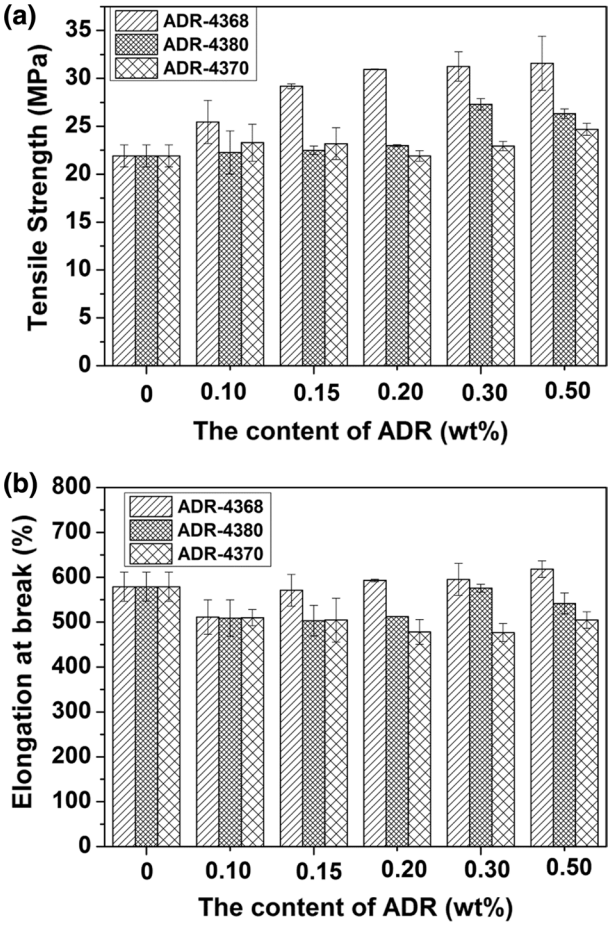

Fig. 5 Tensile properties of the PBAT/PLA blends as a function of different types of ADR

[33] and long chain of the ester groups in the PBAT [43] and PLA [44]. Both effects increased the entanglement density, thus improving the tensile strength. The tensile strength of the PBAT/PLA/0.15ADR4368 blend increased obviously from 21.9 MPa for PBAT/PLA blend to 29.2 MPa. When further increasing the ADR4368 content, the tensile strength and elongation at break of PBAT/PLA/0.2ADR4368 blend were 31.0 MPa and 592.9%. The significant increase in tensile strength of the PBAT/PLA/ADR4368 blends was in agreement with the result of GPC and DSC, which indicated clearly chain extension effect and compatibilization effect, respectively. Further increasing the content of ADR4368, the tensile strength and elongation at break increased slightly. This may be due to the saturation effect of chain extender. The excess compatibilizer was difficult to reach the interface, and it may trap in one of the phases. The tensile strength of PBAT/PLA/ADR4380 blends and PBAT/PLA/ADR4370 blends was higher than PBAT/PLA blend except for the

PBAT/PLA/0.2ADR4370 blend, but the elongation at break was lower than the corresponding PBAT/PLA blend. This reason can be explained by the insufficient multifunctional epoxy groups of ADR4380 and ADR4370, which did not generate sufficient amount of PBAT-*g*-PLA copolymers around the PLA dispersed phase. It cannot transfer the stress effectively under loading and further hindered the mobility of the macromolecular chains of PBAT, thereby contributing to the reduction in the elongation at break. In addition, because of the no valid compatibility of the PBAT and PLA, the enhanced tensile strength was limited. This was consisted with GPC and DSC analysis. The M_n and compatibility of PBAT/PLA/ADR4380 blends and PBAT/PLA/ADR4370 blends were lower than that of PBAT/PLA/ADR4368 blends. However, elongation at break of these PBAT/PLA4380 blends and PBAT/PLA/ADR4370 blends all still remained a high elongation at break, which almost 500%. In sum, from mechanical properties results, the compatibilized PBAT/PLA blend containing 0.2 wt% of ADR4368 had a good balanced properties among all the blends.

Rheological properties

The melt rheology properties are closely related to chain architecture, phase morphology and interfacial actions. According to the above analysis, the PBAT/PLA/ADR4368 blends demonstrated the good compatibility and mechanical properties. Herein, we further studied the melt rheological properties of PBAT/PLA/ADR4368 blends. The dynamic storage modulus (G'), loss modulus (G'') and the complex viscosity (η^*) as a function of ADR4368 content are shown in Fig. 6.

It was clearly observed that G′ and G″ increased with increasing ADR4368 content over the entire frequency range. For example, at an angular frequency of 10 rad/s, the G' of PBAT/PLA blend was 36,470 Pa, which enhanced to 50,530 Pa for the PBAT/PLA/0.2ADR4368 blend. This was expected as a result that the epoxide functions of ADR4368 reacted with the –COOH and –OH groups forming the copolymer which increased the melt strength. The similar results were also reported in the previous research [33, 42]. The higher G' of the melts with the increase of ADR4368 content obviously indicated a further increased entanglement density. The G'' curves exhibited similar trends as the G'. For all the samples, G'' was always higher than G' at any angular frequency meaning all the samples had dominant viscous behavior with long relaxation times at the melting state. The η^* of the PBAT/PLA/ADR4368 blends increased, and the non-Newtonian behavior became more pronounced with increasing ADR4368 content. According to the entanglement theory, the presence of long chain branching structure exacerbated the tangles of the molecular chains, so the η^* increased.

Figure 7 shows the effect of ADRs on the dynamic η^* of PBAT/PLA blend and the PBAT/PLA/0.2ADR blends. The pure PLA melt displayed a Newton liquid behavior at the low-frequency range of ~ 0.5–2 rad/s, and then the shear thinning behavior happened with the frequency increase. The η^* of pure PLA reduced when the frequency was lower than ~ 0.5 rad/s due to the melt subjected to be thermal degradation for a long period of heating measurement. The pure PBAT also showed a

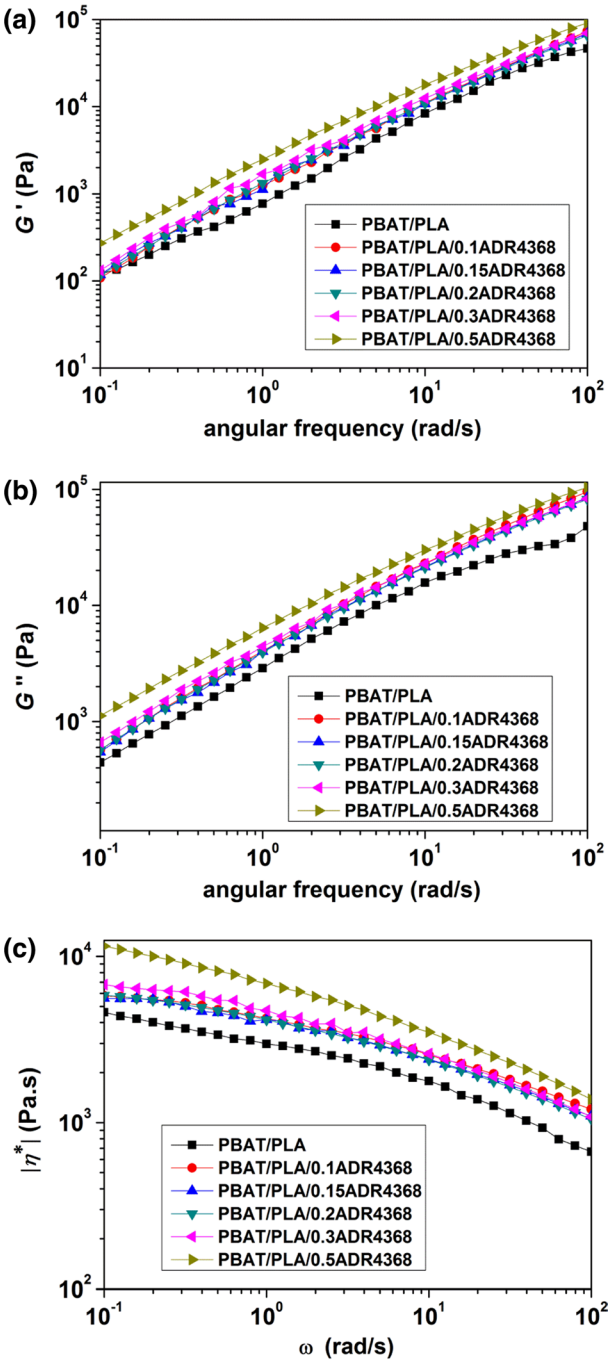

Fig. 6 Deduced frequency dependence of **a** $G'(\omega)$ **b** $G''(\omega)$ and **c** $\eta^*(\omega)$ of PBAT/PLA and PBAT/PLA/ADR4368 blends ($T = 170$ °C)

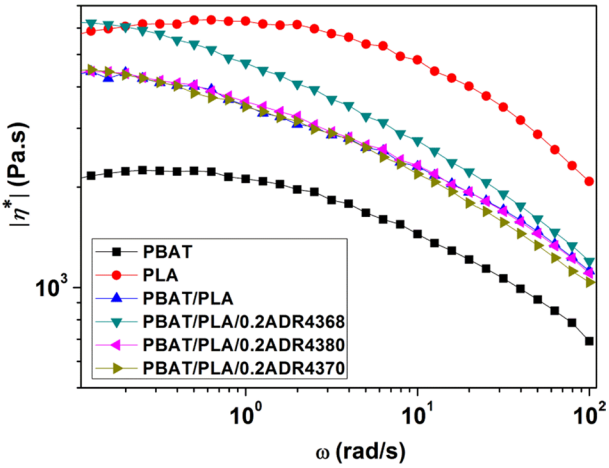

Fig. 7 η^* versus frequency curves for PBAT, PLA, PBAT/PLA blend, PBAT/PLA/0.2ADR4368 blend, PBAT/PLA/0.2ADR4380 blend and PBAT/PLA/0.2ADR4370 blend at 170 °C

short plateau between 0.3 and 0.6 rad/s and a slight decrease at the low-frequency region also indicating the thermal degradation happened. PBAT had a much lower η^* than that of PLA. This resulted from the fact that PLA had a much higher molecular weight than PBAT which was easier to entangle. As expected, the η^* of PBAT/PLA blend was located at between pure PBAT and pure PLA because of the melt blending. It was clear that the η^* of PBAT/PLA/ADR4368 blends increased significantly in the whole frequency region and the PBAT/PLA/ADR4368 blends showed a remarkable shear thinning behavior at high frequency. This was related to the branching structure. However, the η^* of PBAT/PLA/ADR4380 and PBAT/PLA/ADR4370 blends showed no obvious difference with that of the PBAT/PLA blend, meaning that the chain extension effect was limited with low ADR4380 and ADR4370 content. This result revealed that ADR4368 was more effective as a chain extender in comparison with ADR4380 and ADR4370. The rheological analysis was consistent with GPC result.

The temperature dependence of the η^* of polymer melt is one of the most important parameters in polymer flow. In a certain range of temperature, the dependence of the viscosity–temperature behavior can be expressed in the Arrhenius form, $\eta = Ae^{Ea/RT}$ where η is the viscosity, R is the gas constant, A is a constant, E_a is called the flow activation energy (E_a). The higher the E_a, the more temperature sensitive is the melt [23].

The η^* of the PBAT/PLA blend and PBAT/PLA/0.2ADR blends, vs frequency at temperatures of 160, 170, 180 and 190 °C is shown in Fig. 8. The E_a of the blends was calculated through linear regression of $\ln(\eta^*)$ plotted vs $1/T$ at different frequency, shown in Fig. 9. For all samples, the η^* decreased with the increase of temperature and the samples exhibited shear thinning phenomenon. E_a of viscous flow was calculated through Arrhenius fit. The calculated results are listed in Table 3. For all of the samples, the E_a of viscous flow at high frequencies

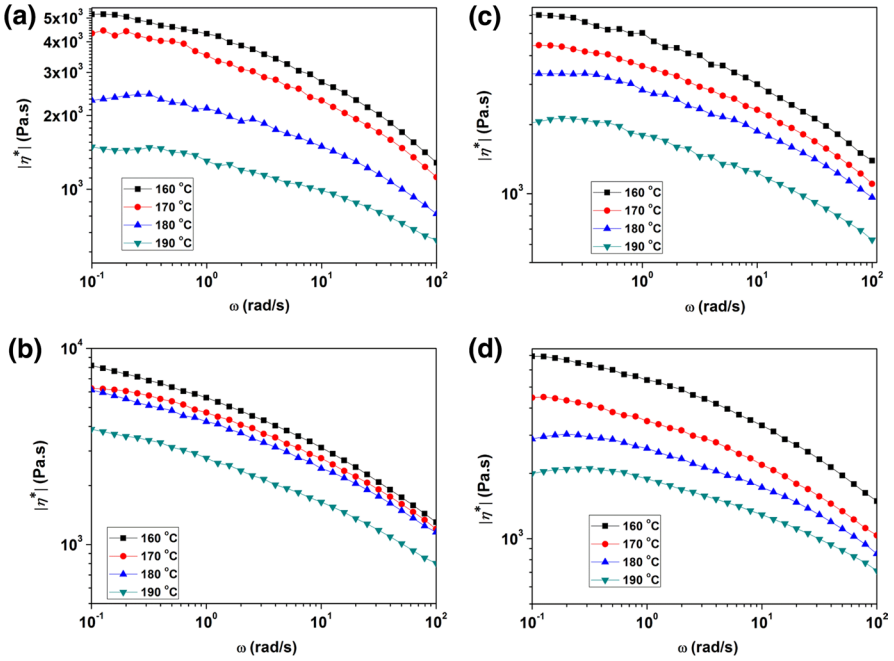

Fig. 8 η^* versus frequency curves for the blend: **a** PBAT/PLA blend, **b** PBAT/PLA/0.2ADR 4368 blend, **c** PBAT/PLA/0.2ADR4380 blend and **d** PBAT/PLA/0.2ADR4370 blend

was smaller than that at lower frequencies. This illustrated that higher shearing rate can decrease the E_a and facilitate the viscous flow.

The E_a was significantly affected by the presence of long chain branching. Dorgan et al. reported that the E_a was independent of molecular weight and was only dependent on the local segmental nature of the chain. The literature attributed these discrepancies in E_a of linear and branched polymers to whether or not the branches formed a stable entanglement network [45]. In this work, the E_a of PBAT/PLA/ADR blends tended to decrease. The architecture of the polymer, molecular weight distribution and shear rate can affect the E_a. PLA molecular chain contained side group, which was rigid and had poor fluidity, while PBAT molecular chain had good flexibility and fluidity. With the introduction of branched structure, the mobile PBAT promoted the movement of PLA chain segment, thus reducing the E_a. On the other hand, the less temperature dependence of η^* of PBAT/PLA melts made it easier for choosing of processing temperatures.

At a given oscillatory shear frequency, the E_a of PBAT/PLA/ADR4368 blend was lower than that of PBAT/PLA/ADR4380 and PBAT/PLA/ADR4370 blend. This indicated that PBAT/PLA/ADR4368 melt had lower temperature sensibility than PBAT/PLA/ADR4380 and PBAT/PLA/ADR4370 melt due to more branching chains.

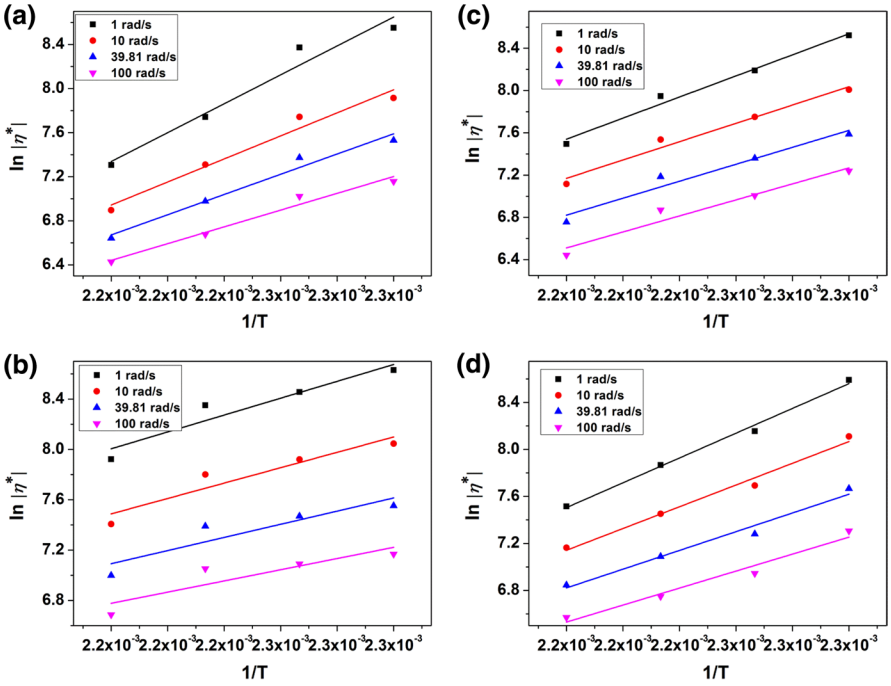

Fig. 9 ln |η*| versus 1/T curves for the blend: **a** PBAT/PLA, **b** PBAT/PLA/0.2ADR4368, **c** PBAT/PLA/0.2ADR4380 and **d** PBAT/PLA/0.2ADR4370 at different frequencies

Table 3 E_a of viscous flow of PBAT/PLA blend, PBAT/PLA/ADR blends at different frequencies

Samples	E_a (kJ/mol)			
	1 rad/s	10 rad/s	39.81 rad/s	100 rad/s
PBAT/PLA	67.94	57.93	50.87	42.15
PBAT/PLA/0.2ADR4368	37.13	33.87	28.95	24.66
PBAT/PLA/0.2ADR4380	55.27	48.02	44.45	41.99
PBAT/PLA/0.2ADR4370	58.48	51.28	44.20	40.07

Morphological characterization

Figure 10 compares the morphology of PBAT/PLA/ADR4368 blends, and morphology was closely related to mechanical properties. PBAT and PLA are thermodynamic immiscible polymer pairs, usually inducing the phase separation [46]. In Fig. 10a, as expected, the PBAT/PLA blend exhibited a typical matrix-dispersed phase morphology with the spherical PLA droplets. The PLA phase was dispersed non-uniformly in the PBAT matrix with uneven domain size (~ 1.0 μm), and adhesion between the PLA and PBAT phases was poor as evidenced by an obvious interfacial debonding and oval cavities left by the PLA domains after cryo-fracture. For

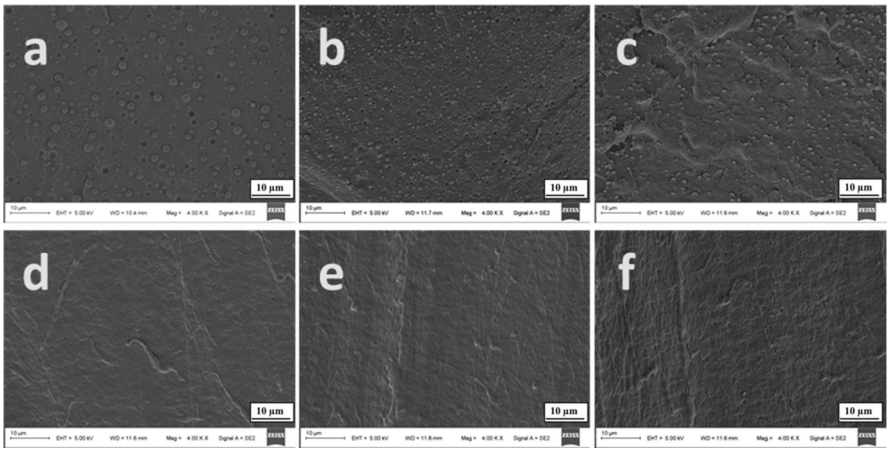

Fig. 10 SEM images of the cryo-fractured surfaces of the blends **a** PBAT/PLA, **b** PBAT/PLA/0.1ADR4368, **c** PBAT/PLA/0.15ADR4368, **d** PBAT/PLA/0.2ADR4368, **e** PBAT/PLA/0.3ADR4368, **f** PBAT/PLA/0.5ADR4368

the PBAT/PLA/0.1ADR4368 blend, the dispersion of the PLA domains became uniform and the average PLA domain size reduced to approximately 0.63 µm. The amount of dispersed domains of PLA further decreased and phase interface became indistinct for the PBAT/PLA/0.15ADR4368 blend. The interfacial adhesion between PLA and PBAT was enhanced after the incorporation of ADR4368 due to the formation of PLA-*g*-PBAT copolymers. A weakening of morphological features was observed when further increasing the content of ADR4368. In particular, for the PBAT/PLA/0.2ADR4368 blend, the interface becomes less distinguishable suggesting a significant compatibilization effect. These results contributed to the increasing trend of tensile strength. With increasing the ADR4368 content, the PLA phase became vague (Fig. 10e and f) implying a strong interfacial adhesion. These results prove that in situ compatibilization was created in the PLA/PBAT blends [36].

It is well known that mixing immiscible polymers often results in a heterogeneous dispersion and poor mechanical properties. A suitable block copolymer (linear or graft) acted as an emulsifier leading to a finer morphology with improved interphase adhesion and mechanical properties. The dispersed phase size was evolutive as increasing the compatibilizer content. There was a minimum amount of compatibilizer needed to saturate the interface in the melt blending of immiscible polymer blends. The interfacial saturation referred to the point where the dispersed particle size was no longer significantly dependent on the amount of interfacial agent. That was to say, the dispersed phase size was almost unchanged when the compatibilizer content was beyond the critical value of the concentration of the compatibilizer.

In this work, the emulsification data from the SEM images are plotted in Fig. 11. The small concentration of ADR4368 led to decrease the dispersed phase size and increase the stability of the dispersion. The branching copolymer accumulated at the interface, giving rise to a pronounced decrease of the interfacial tension. With increasing the ADR4368 content, the dispersed phase disappeared corresponding to

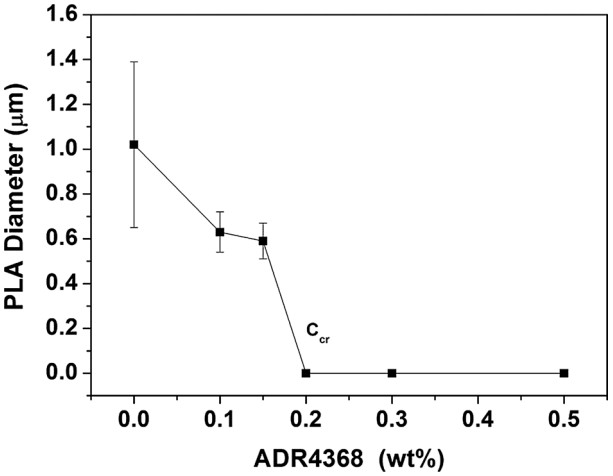

Fig. 11 Schematic drawing of a typical emulsification curve where the critical concentration C_{cr} was related to interfacial saturation

the equilibrium region in the emulsification curve. The critical concentration for the interfacial saturation can be identified at 0.2 wt% of ADR4368. When the ADR4368 content was outside the threshold, the branching copolymers became more difficult to go to the interface, and they remained randomly entrapped in one of the phases or it will form micellar structures with other block copolymer chains.

Figure 12 shows that the ADR4368 can react with a component polymer of PBAT and PLA during melt mixing to form double graft/comb copolymers. The two side chains are not miscible with each other, so reactive blending may form so-called Janus micelles located exclusively at the interface between the two phases. The PBAT and PLA side chains penetrated into the PBAT and PLA phase, respectively. This can efficiently decrease the interfacial tension, inhibit coalescence of the dispersed phase and ultimately improve interfacial adhesion. These effects contributed

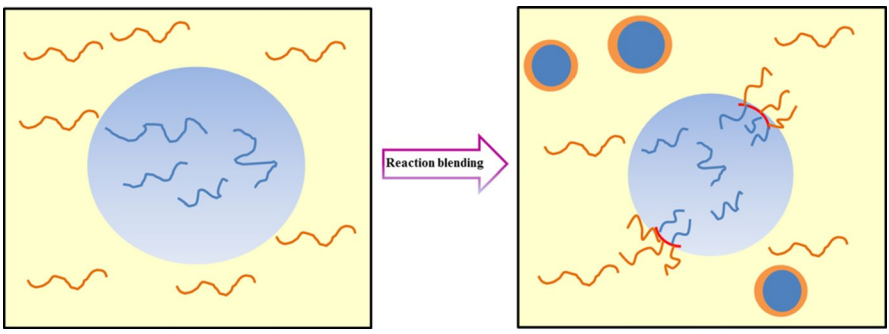

Fig. 12 Schematic diagrams of the in situ formation of PBAT-*g*-PLA copolymers at the interface of immiscible PBAT/PLA blend and the morphology development of binary blends by reactive blending

to decrease the phase size and increase the stability of the dispersion. Particularly, the double graft/comb copolymers were more effective to improve the compatibility of immiscible polymer blends.

Thermal stability

The TGA curves of pure PBAT, PLA, PBAT/PLA blend and PBAT/PLA/ADR blends are shown in Fig. 13. Table 4 summarizes the TGA data of the onset degradation temperature (T_5, the temperature at which 5 wt% weight loss occurred) and for the maximum rate of weight loss (T_{max}). For the PBAT and PLA, a single-step decomposition process was observed. Pure PLA degraded from 320 to 354 °C, while pure PBAT degraded from 375 to 549 °C. PBAT was more thermally stable than PLA due to the higher thermal resistance of aromatic rings in the molecular structure of PBAT. However, in the case of PBAT/PLA blend, the curve displayed two degradation steps. The first decomposition stage corresponded to degradation of PLA, and the second decomposition stage was related to the degradation of the PBAT. The thermal degradation of PBAT/PLA blend started at around 321 °C and ended at about 500 °C. The PBAT/PLA/ADR4368 blend also exhibited a two-step decomposition process, but the thermal degradation steps shifted closer to each other compared with the PBAT/PLA blend, thereby suggesting the improved compatibility as a result of the afore-mentioned PLA-*g*-PBAT copolymer formation by the addition of ADR4368. In addition, the T_5 of the PBAT/PLA/0.5ADR4368 blend was 316 oC that was slightly lower than that of PBAT/PLA blend. This can be explained by the low thermal stability of the ADR4368.

According to the data analysis in Table 4, it showed PBAT/PLA/0.2ADR4368 had a higher thermal stability than PBAT/PLA/0.2ADR4380 blend and PBAT/PLA/0.2ADR4370 blend which was attributed to the effective branching reaction between PBAT and PLA, which increased the thermal stability.

Conclusion

In this work, the ADRs were used in order to improve the compatibility and the properties of PBAT/PLA blends by reactive melt blending. The ^{1}H NMR study showed that the main structure of different ADRs was similar, but the amount of epoxy group of ADRs was different. Thermal properties, GPC, mechanical properties, rheological behavior, morphology and the thermal stability of the PBAT/PLA/ADR blends were investigated in detail. The modification effect had the following sequence: ADR4368 > ADR4380 > ADR4370. When the addition content of ADR was 0.5wt%, the M_n of PBAT/PLA/ADR4368, PBAT/PLA/ADR4380 and PBAT/PLA/ADR4370 increased to 97,071, 90,716 and 87,923 due to the chain extension after addition ADRs. At the same time, the corresponding tensile strength from 21.9 MPa for PBAT/PLA blend increased to 31.6 MPa, 26.3 MPa and 24.7 MPa, respectively. ADR4368 was more effective as chain extender for producing plenty of PBAT-*g*-PLA copolymers, which contributed to the increasing tensile properties.

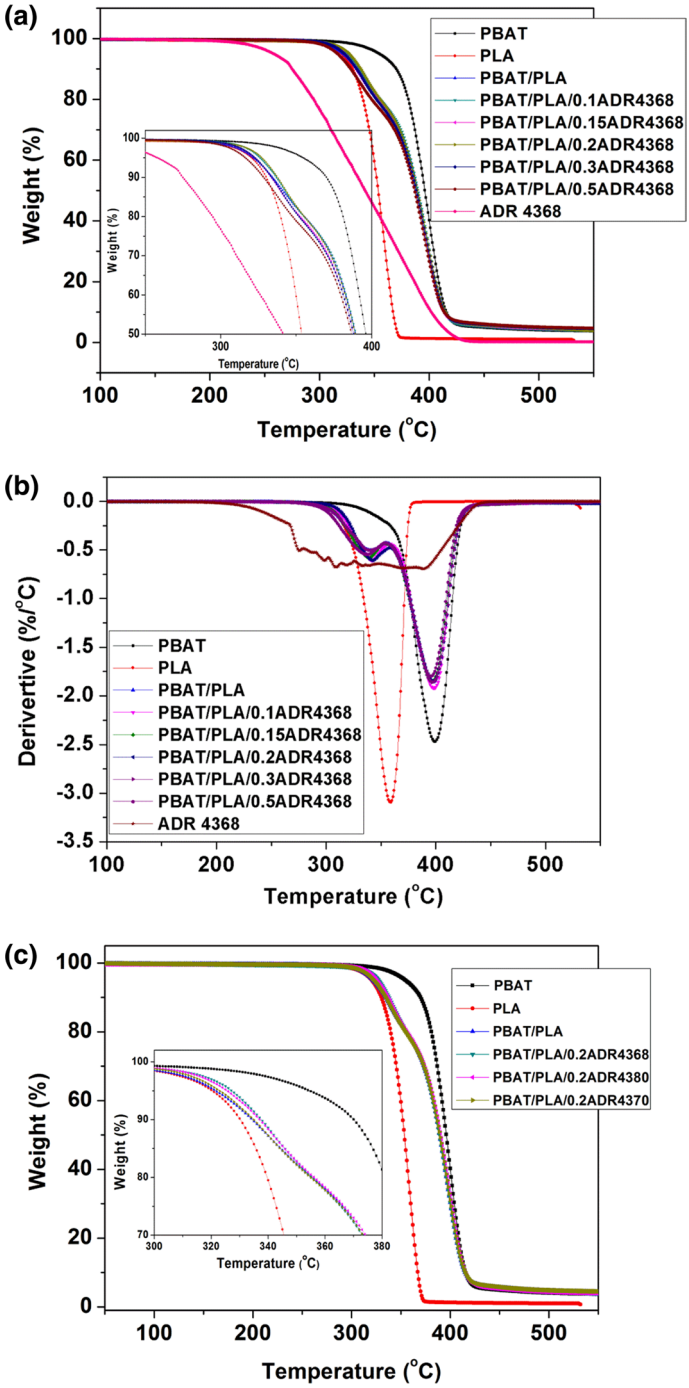

Fig. 13 The thermal stability of the biodegradable blends

Table 4 Character temperatures of PBAT, PLA, PBAT/PLA blend and PBAT/PLA/ADR blends obtained from TGA and DTA curves

Samples	$T-_{5\%}$ (°C)	$T^1{}_{max}$ (°C)	$T^2{}_{max}$ (°C)
PBAT	354.0	–	399.1
PLA	320.2	359.0	–
PBAT/PLA	321.2	336.6	397.1
PBAT/PLA/0.1ADR4368	326.4	340.5	399.0
PBAT/PLA/0.15ADR4368	322.5	337.5	397.1
PBAT/PLA/0.2ADR4368	326.3	341.1	398.2
PBAT/PLA/0.3ADR4368	323.1	339.0	397.7
PBAT/PLA/0.5ADR4368	326.4	334.1	396.0
PBAT/PLA/0.2ADR4380	327.3	340.7	399.2
PBAT/PLA/0.2ADR4370	326.0	338.0	398.4

$T^1{}_{max}$ and $T^2{}_{max}$ were denoted as the thermal decomposition temperature with the max rate of the PLA-rich phase and PBAT-rich phase, respectively

The ductility of PBAT/PLA blends also remained a high value after incorporation ADRs. The complex viscosity of the PBAT/PLA/ADR4368 blend had the highest values at the whole measured angular frequency range among the PBAT/PLA/ADR blends. ADR4368 could improve the intermolecular entanglement of the PLA/PBAT blends significantly. The storage modulus, loss modulus and complex viscosity of the PBAT/PLA blends increased with increasing ADR4368 content. The E_a of PBAT/PLA/ADR blends tended to decrease compared with PBAT/PLA blend, and the E_a of PBAT/PLA/ADR4368 blend was lower than that of PBAT/PLA/ADR4380 and PBAT/PLA/ADR4370 blend, indicating that PBAT/PLA/ADR4368 melt had low-temperature sensibility. A small amount of the ADR4368 increased the compatibility of the blends obviously as evidenced by a reduction of the PLA domain size and enhanced in the interfacial adhesion in SEM observation. Moreover, thermal stability of blends was enhanced with addition of ADR. The better compatibility of PBAT/PLA blends, the higher thermal stability of PBAT/PLA blends. These results may be of significant and important for the wider practical application for the PBAT/PLA blend.

Compliance with ethical standards

Conflict of interest The authors declare that they have no conflict of interest.

References

1. Li YD, Fu QQ, Wang M, Zeng JB (2017) Morphology, crystallization and rheological behavior in poly(butylenesuccinate)/cellulose nanocrystal nanocomposites fabricated by solution coagulation. Carbohydr Polym 164(15):75–82

2. Saeidlou S, Huneault MA, Li H, Park CB (2012) Poly(lacticacid) crystallization. Prog Polym Sci 37(12):1657–1677
3. Raquez JM, Habibi Y, Murariu M, Dubois P (2013) Polylactide (PLA)-based nanocomposites. Prog Polym Sci 38(10–11):1504–1542
4. Schneider J, RamaniNaray SM (2016) An reactive modification and compatibilization of poly(lactide)and poly(butylene adipate-co-terephthalate) blends with epoxy functionalized-poly(lactide) for blown film applications. J Appl Polym Sci. https://doi.org/10.1002/app.43310
5. Wang DM, Yu YL, Ai X, Pan HW, Zhang HL, Dong LS (2019) Polylactide/poly(butylene adipate-co-terephthalate)/rare earth complexes as biodegradable light conversion agricultural films. Polym Adv Technol 30(1):203–211
6. Nampoothiri KM, Nair NR, John RP (2010) An overview of the recent developments in polylactide (PLA) research. Bioresour Technol 101(22):8493–8501
7. Jiang L, Wolcott MP, Zhang JW (2006) Study of biodegradable polylactide/poly(butylene adipate-co-terephthalate) blends. Biomacromol 7(1):199–207
8. Martin O, Averous L (2001) Poly(lactic acid): plasticization and properties of biodegradable multiphase systems. Polymer 42(14):6209–6219
9. Jacobsen S, Fritz HG (1999) Plasticizing polylactide: the effect of different plasticizers on the mechanical properties. Polym Eng Sci 39(7):1303–1310
10. Kulinski Z, Piorkowska E, Gadzinowska K, Stasiak M (2006) Plasticization of poly(L-lactide) with poly(propylene glycol). Biomacromol 7(7):2128–2135
11. Ji LJ, Gong MD, Qiao W, Zhang WQ, Liu QR, Dunham RE, Gu J (2018) A gelatin/PLA-b-PEG film of excellent gas barrier and mechanical properties. J Polym Res 25(10):210–222
12. Kim JK, Park DJ, Lee MS, Ihn KJ (2001) Synthesis and crystallization behavior of poly(L-lactide)-b-poly(e-caprolactone) copolymer. Polymer 42(17):7429–7441
13. Ding Y, Lu B, Wang PL, Wang GX, Ji JH (2018) PLA-PBAT-PLA tri-block copolymers: effective compatibilizers for promotion of the mechanical and rheological properties of PLA/PBAT blends. Polym Degrad Stabil 147(8):41–48
14. Ding Y, Feng WT, Lu B, Wang PL, Wang GX, Ji JH (2018) PLA-PEG-PLA tri-block copolymers: effective compatibilizers for promotion of the interfacial structure and mechanical properties of PLA/PBAT blends. Polymer 146(20):179–187
15. Wang RY, Wang SF, Zhang Y, Wan CY, Ma PM (2009) Toughening modification of PLLA/PBS blends via in situ compatibilization. Polym Eng Sci 49(1):26–33
16. Farsetti S, Cioni B, Lazzeri A (2011) Physico-mechanical properties of biodegradable rubber toughened polymers. Macromol Symp 301(1):82–89
17. Broz ME, VanderHart DL, Washburn NR (2003) Structure and mechanical properties of poly(d, l-lactic acid)/poly(e-caprolactone) blends. Biomaterials 24(23):4181–4190
18. Semba T, Kitagawa K, Ishiaku US, Hamada H (2006) The effect of crosslinking on the mechanical properties of polylactic acid/polycaprolactone blends. J Appl Polym Sci 101(3):1816–1825
19. Li Y, Shimizu H (2007) Toughening of polylactide by melt blending with a biodegradable poly(ether) urethane elastomer. Macromol Biosci 7(7):921–928
20. Zhang W, Chen L, Zhang Y (2009) Surprising shape-memory effect of polylactide resulted from toughening by polyamide elastomer. Polymer 50(5):1311–1315
21. Jaratrotkamjorn R, Khaokong C, Tanrattanakul V (2012) Toughness enhancement of poly(lactic acid) by melt blending with natural rubber. J Appl Polym Sci 124(6):5027–5036
22. Hongdilokkul P, Keeratipinit K, Chawthai S, Hararak B, Seadan M, Suttiruengwong S (2015) A study on properties of PLA/PBAT from blown film process. Mat Sci Eng 87(12):012–112
23. Gu SY, Zhang K, Ren J, Zhan H (2008) Melt rheology of polylactide/poly(butylene adipate-co-terephthalate) blends. Carbohydr Polym 74(1):79–85
24. Chiu HT, Huang SY, Chen YF, Kuo MT, Chiang TY, Chang CY, Wang YH (2013) (2013) Heat treatment effects on the mechanical properties and morphologies of poly (lactic acid)/poly (butylene adipate-co-terephthalate) blends. Int J of Polym Sci 15:1–11
25. Imre B, Pukánszky B (2013) Compatibilization in bio-based and biodegradable polymer blends. Eur Polym J 49(6):1215–1233
26. Zhang M, Thomas NL (2011) Blending polylactic acid (PLA) with polyhydroxybutyrate (PHB): the effect on thermal, mechanical and biodegradation properties. Adv Polym Technol 30(2):67–79
27. Yeh JT, Tsou CH, Huang CY, Chen KN, Wu CS, Chai WL (2010) Compatible and crystallization properties of poly(lacticacid)/poly(butylene adipate-co-terephthalate) blends. J Appl Polym Sci 116(2):680–687

28. Weng YX, Jin YJ, Meng QY, Wang L, Zhang M, Wang YZ (2013) Biodegradation behavior of poly(butylene adipate-co-terephthalate) (PBAT), poly(lactic acid) (PLA), and their blend under soil conditions. Polym Test 32(5):918–926
29. Deng YX, Yu CY, Wongwiwattana P, Thomas NL (2018) Optimising ductility of poly(lactic acid)/poly(butylene adipate-co-terephthalate) blends through co-continuous phase morphology. J Polym Envir 26(8):3802–3816
30. Lin S, Guo W, Chen C, Ma J, Wang B (2012) Mechanical properties and morphology of biodegradable poly(lactic acid)/poly(butyleneadipate-co-terephthalate) blends compatibilized by transesterification. Mater Des 36:604–608
31. Ma P, Hristova-Bogaerds DG, Lemstra PJ, Zhang Y (2012) Toughening of PHBV/PBS and PHB/PBS blends via in situ compatibilization using dicumyl peroxide as a free-radical grafting initiator. Macromol Mater Eng 297(5):402–410
32. Signori F, Boggioni A, Righetti MC, Rondán CE, Bronco S, Ciardelli F (2015) Evidences of transesterification, chain branching and cross-linking in a biopolyester commercial blend upon reaction with dicumyl peroxide in the melt. Macromol Mater Eng 300(2):153–160
33. Al-Itry R, Lamnawar K, Maazouz A (2012) Improvement of thermal stability, rheological and mechanical properties of PLA, PBAT and their blends by reactive extrusion with functionalized epoxy. Polym Degrad Stab 97(10):1898–1914
34. Al-Itry R, Lamnawar K, Maazouz A, Billon N, Combeaud C (2015) Reactive extrusion of PLA, PBAT with a multi-functional epoxide: physico-chemical and rheological properties. Eur Polyme J 68:288–301
35. Dong W, Zou B, Yan Y, Ma P, Chen M (2013) Effect of chain-extenders on the properties and hydrolytic degradation behavior of the poly (lactide)/poly (butylene adipate-co-terephthalate) blends. Int J Mol Sci 14(10):20189–20203
36. Ma P, Cai X, Zhang Y, Wang S, Dong W, Chen M, Lemstra PJ (2014) In-situ compatibilization of poly(lactic acid) and poly(butyleneadipate-co-terephthalate) blends by using dicumyl peroxide as a free-radical initiator. Polym Degrad Stab 102(15):145–151
37. Kumar M, Mohanty S, Nayak SK, RahailParvaiz M (2010) Effect of glycidyl methacrylate (GMA) on the thermal, mechanical and morphological property of biodegradable PLA/PBAT blend and its nanocomposites. Bioresour Technol 101(21):8406–8415
38. Zhang NW, Zeng C, Wang L (2013) Preparation and properties of biodegradable poly(lactic acid)/poly(butylene adipate-co-terephthalate) blend with epoxy functional styrene acrylic copolymer as reactive agent. J Polym Environ 21(10):286–292
39. Abdelwahaby MA, Taylor S, Misra M, Mohanty AK (2015) Thermo-mechanical characterization of bioblends from polylactide and poly(butyleneadipate-co-terephthalate) and lignin. Macromol Mater Eng 300(3):299–311
40. de Nunes ECD, de Souza AG, Rosa DS (2019) Effect of the Joncryl1 ADR compatibilizing agent in blends of poly(butylene adipate-co-terephthalate)/poly(lactic acid). Macromol Symp 383(1):1800035
41. Costa ARM, Almeida TG, Silva SML, Carvalho LH, Canedo EL (2015) Chain extension in poly(butylene-adipate-terephthalate) Inline testing in a laboratory internal mixer. Polym Test 42(5):115–121
42. Al-Itry R, Lamnawar K, Maazouz A (2014) Reactive extrusion of PLA, PBAT with a multi-functional epoxide: physico-chemical and rheological properties. Eur Polym J 58(8):90–102
43. Song JS, Zhou HF, Wang XD, Zhang YX, Mi JG (2018) Role of chain extension in the rheological properties, crystallization behaviors, and microcellular foaming performances of poly (butylene adipate-co-terephthalate). J Appl Polym Sci 136(14):1–10
44. Wang LY, Jing XB, Cheng HB, Hu XL, Yang LX, Huang YB (2012) Blends of linear and long-chain branched poly(L-lactide)s with high melt strength and fast crystallization rate. Ind Eng Chem Res 51(30):10088–10099
45. Dorgan JR, Williams JS, Lewis DN (1999) Melt rheology of poly(lactic acid):entanglement and chain architecture effects. J Rheol 43(5):1141–1155
46. Long J, Michael PW, Zhang J (2006) Study of biodegradable polylactide/poly(butylenesadipate-co-terephthalate) blends. Biomacromol 7(1):199–207